Pamukkale Univ Muh Bilim Derg, 31(8), 1494-1504, 2025
(Special Issue of the 10th Geochemistry Symposium)

Pamukkale Üniversitesi Mühendislik Bilimleri Dergisi

Pamukkale University Journal of Engineering Sciences

P-T evolution of subophiolitic amphibolites beneath the Kınık Ophiolite (İAESZ, Türkiye): Insights from garnet and amphibole chemistry

Kınık Ofiyoliti (İAESZ, Türkiye) altındaki subofiyolitik amfibolitlerin P-T evrimi: Granat ve amfibol kimyasından bulgular

İrem Aksoy[1*]

[1]Department of Geological Engineering, Faculty of Engineering, Dumlupınar University, Kütahya, Türkiye.
irem.arat@dpu.edu.tr

Received/Geliş Tarihi: 14.09.2025 Revision/Düzeltme Tarihi: 04.11.2025 doi: 10.65206/pajes.87262
Accepted/Kabul Tarihi: 07.11.2025 Special Issue Article/Özel Sayı Makalesi

Abstract

The metamorphic sole rocks at the base of the Kınık Ophiolite in the İzmir-Ankara-Erzincan Suture Zone provide important insights into the tectonothermal evolution of the northern Neotethys. Field and petrographic observations reveal a sequence of amphibolites, garnet-amphibolites, amphibole schists, and quartz schists, displaying granoblastic to nematoblastic textures with retrograde overprinting by chlorite and epidote. Mineral chemical data show that garnets are dominated by almandine with subordinate pyrope and grossular, and very low spessartine, consistent with basaltic protoliths. Amphiboles are mainly calcic types, such as magnesiohornblende and tschermakite, preserving magmatic affinities but partly modified during metamorphism. Geothermobarometric calculations indicate peak conditions of ~640-790 °C and ~4-5 kbar, corresponding to medium- to upper-amphibolite facies at mid-crustal depths of ~14-20 km. The higher temperatures recorded in one sample suggest a low-pressure/high-temperature regime, typical of metamorphic soles. These findings demonstrate that the Kınık amphibolites originated from basaltic precursors and underwent LP-HT metamorphism during intra-oceanic subduction and subsequent ophiolite emplacement.

Keywords: Kınık Ophiolite, Subophiolitic metamorphic sole, Amphibolite facies, Garnet-hornblende geothermometry, Al-in-hornblende barometry, Neotethys closure.

Öz

İzmir-Ankara-Erzincan Sütur Zonu'nda yer alan Kınık Ofiyoliti'nin tabanındaki metamorfik taban kayaçları, kuzey Neotetis'in tektono-termal evrimi hakkında önemli bilgiler sunmaktadır. Arazi ve petrografik gözlemler; amfibolit, granat-amfibolit, amfibolşist ve kuvarsşistlerden oluşan bir diziyi ortaya koymakta olup, bu kayaçlar granoblastik ve nematoblastik dokular sergilemekte ve klorit ile epidot tarafından temsil edilen retrograd etkilerle değişim göstermektedir. Mineral kimyası verileri granatların baskın olarak almandin, daha az oranda pirop ve grossular, çok düşük oranda ise spessartin içerdiğini ve bazaltik protolitlerle uyumlu olduğunu göstermektedir. Amfiboller ise çoğunlukla kalsik tiplerdir (magnezyohornblend ve çermakit) ve kısmen metamorfizma ile yeniden dengelenmiş olsalar da magmatik özelliklerini büyük ölçüde korumaktadır. Jeotermobarometrik hesaplamalar, yaklaşık 640-790 °C sıcaklık ve 4-5 kbar basınç koşullarını işaret etmektedir. Bu değerler orta-üst amfibolit fasiyesi koşullarına ve yaklaşık 14-20 km derinliklere karşılık gelmektedir. Özellikle bir örnekte kaydedilen daha yüksek sıcaklıklar, metamorfik tabanlara özgü düşük basınç-yüksek sıcaklık (LP-HT) rejimine işaret etmektedir. Bu bulgular, Kınık amfibolitlerinin bazaltik protolitlerden türediğini ve okyanus içi dalma-batma sırasında, ofiyolit yerleşimi esnasında LP-HT metamorfizmasına uğradığını ortaya koymaktadır.

Anahtar Kelimeler: Kınık Ofiyoliti, Subofiyolitik metamorfik taban, Amfibolit fasiyesi, Granat-hornblend jeotermometresi, Al-in-hornblend jeobarometresi, Neotetis'in kapanışı.

1 Introduction

Ophiolites are major geological units formed by the emplacement of oceanic lithosphere onto continental margins and represent key records for understanding subduction-related processes [1]-[4]. In the context of the Tethyan realm, the formation of these units is strongly associated with the closure of the Neotethys Ocean. In Türkiye, the İzmir-Ankara-Erzincan Suture Zone (İAESZ) represents one of the most important tectonic belts recording the final closure of the northern branch of the Neotethys (Figure 1a, b). This suture zone is characterized by widespread ophiolitic complexes and their associated metamorphic sole rocks, which provide essential constraints on the geodynamic evolution of subduction-accretion systems [5],[6].

At the base of these ophiolitic sequences, subophiolitic metamorphic rocks (metamorphic sole) occur as direct products of metamorphism developed during the tectonic emplacement of ophiolites, thus providing crucial constraints on the pressure-temperature-time paths of suture zones [7]-[11]. These metamorphic units are typically composed of amphibolites, schists, and quartzites. Among them, amphibolites are particularly common and mostly derive from the metamorphism of basaltic protoliths under medium- to high-temperature conditions [5],[6],[12]-[20]. Mineralogically, amphibolites are mainly characterized by assemblages of hornblende+plagioclase±garnet±biotite, which vary according to facies conditions.

Therefore, the study of mineral chemistry and geothermobarometric properties of amphibolites provides not only insights into the metamorphic evolution but also critical information on protolith characteristics and the tectonic development of the metamorphic sole.

*Corresponding author/Yazışılan Yazar

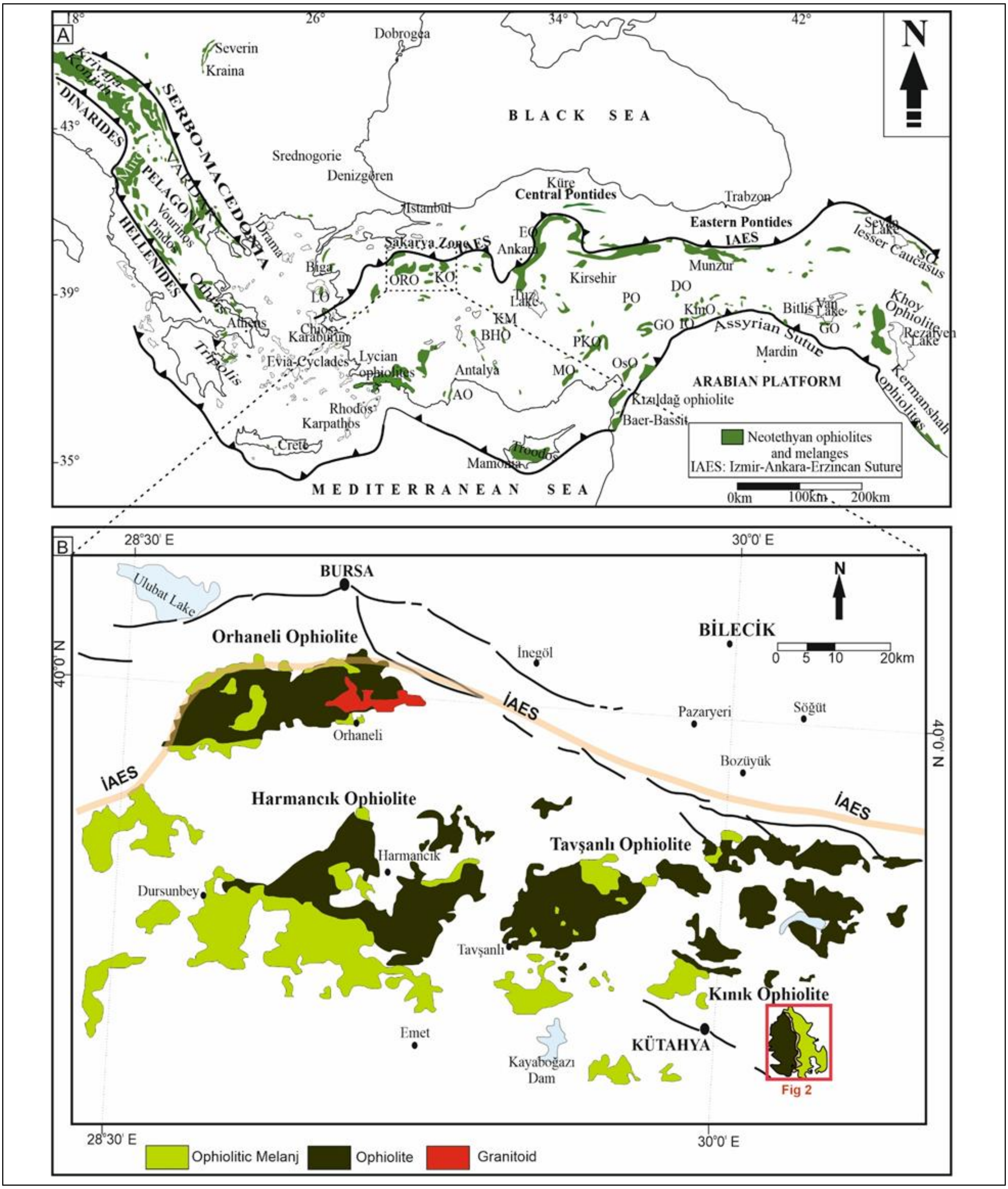

Figure 1. (a): Regional distribution of Neotethyan ophiolites and mélanges in the Eastern Mediterranean, showing the İzmir-Ankara-Erzincan Suture Zone (IAESZ) as a major tectonic boundary (modified after [21],[22]; Green shading marks the main ophiolitic complexes related to the closure of the Neotethys). (b): Simplified map of northwest Türkiye, illustrating the Orhaneli, Harmancık, Tavşanlı, and Kınık ophiolites within the IAESZ. The Kınık Ophiolite (Kütahya) is highlighted as the focus of this study (modified after [23].

Metamorphic sole rocks are widely distributed along the İzmir-Ankara-Erzincan Suture Zone (IAESZ) and provide crucial records of the tectono-thermal evolution associated with the formation and closure of the northern branch of the Neotethys Ocean. Numerous petrological studies have demonstrated that the peak metamorphic conditions recorded in these units are characterized by high-temperature/low-pressure (HT/LP) amphibolite facies metamorphism, generally dated to the Late Cretaceous [14],[20],[24]. These HT/LP conditions are widely interpreted as evidence for rapid ophiolite obduction processes triggered by the initiation of intra-oceanic subduction [4],[20].

Across the IAESZ, metamorphic soles associated with different ophiolitic sequences typically record peak conditions within the amphibolite facies, ranging from 700 to 850 °C and 5 to 8 kbar. For example, metamorphic soles in the Tokat region (northern Türkiye) record HT/LP conditions around 89-91 Ma [24], while similar pressure-temperature conditions have been reported from the Divriği Ophiolite (Sivas)[20] and the Eldivan-Ahlat areas of the Çankırı region [25]. These results collectively indicate a regional HT/LP metamorphic event associated with intra-oceanic subduction processes along the IAESZ.

In contrast, the underlying Tavşanlı Zone represents a continental subduction environment that records high-pressure/low-temperature (HP/LT) metamorphism [26],[27], reflecting the subduction of the northern margin of the Anatolide-Tauride Block during the final closure of Neotethys. Within this tectonic framework, the Kınık Ophiolite constitutes a key area that preserves the record of HT/LP metamorphism. Although early studies [14] reported amphibolite-facies conditions, detailed mineral chemical and thermobarometric data for the Kınık amphibolites remain scarce.

This study aims to determine the metamorphic conditions and protolith characteristics of the subophiolitic amphibolites forming the metamorphic sole of the Kınık Ophiolite. For this purpose, the mineral chemistry of amphibole and garnet was examined, and garnet-hornblende geothermometers [28]-[32] together with the Al-in-hornblende geobarometer [33] were applied to constrain peak metamorphic conditions and to evaluate the protolith nature of these rocks. These new quantitative results are expected to provide additional insights into the metamorphic evolution of the Kınık Ophiolite and refine existing interpretations of obduction processes within the IAESZ.

2 Regional geology

The geological evolution of Türkiye during the Alpine-Himalayan orogeny was strongly influenced by the subduction and closure of the Neotethys Ocean [2]. Several east-west trending ophiolitic belts are preserved across Anatolia, many of which display supra-subduction zone (SSZ) affinities and mark ancient suture zones that record subduction-accretion processes[34]-[36].

The İzmir-Ankara-Erzincan Suture Zone (İAESZ) forms one of the major tectonic boundaries in northern Türkiye, separating the Sakarya Zone in the north from the Anatolide-Tauride block in the south. During the Mesozoic, this zone recorded the northward subduction of the Neotethyan lithosphere and the southward emplacement of ophiolites, accompanied by related thrust systems and north-dipping tectonic fabrics [2],[37], [38]. Within this framework, the Kaynarca area near Kütahya provides one of the most continuous and well-preserved metamorphic sole sequences in Türkiye, where metamorphic grade increases upward from greenschist to amphibolite facies [6],[14].

The regional geology is dominated by the Çöğürler Complex at the base, consisting of an ophiolitic olistostrome with blueschists, pelagic sediments, and neritic carbonates, tectonically overlain by the Kınık Ophiolite, an incomplete mafic-ultramafic sequence [39],[40]. Between these two units, subophiolitic metamorphic rocks, including amphibolites, schists, and garnet-bearing amphibolites, are exposed over ~40 km with thicknesses of 10-150 m [40]. These rocks, derived from basaltic protoliths with OIB-like affinities, record high-temperature/low-pressure metamorphism associated with intra-oceanic thrusting and subsequent subduction [14]. Radiometric data indicate an Albian-Campanian age for metamorphism, with an Ar-Ar age of ~93±2 Ma for the peak HT event [14].

2.1 Field observations

The subophiolitic metamorphic sequence in the study area mainly consists of amphibolites and schists in tectonic contact with serpentinites. The serpentinite-amphibolite boundary is strongly sheared, reflecting intense deformation related to the tectonic emplacement of the ophiolite. Despite extensive forest and agricultural cover, the metamorphic units are well exposed in road cuts between Akoluk village and Kaynarca, as well as around Ürün Çiftliği (Figure 2).

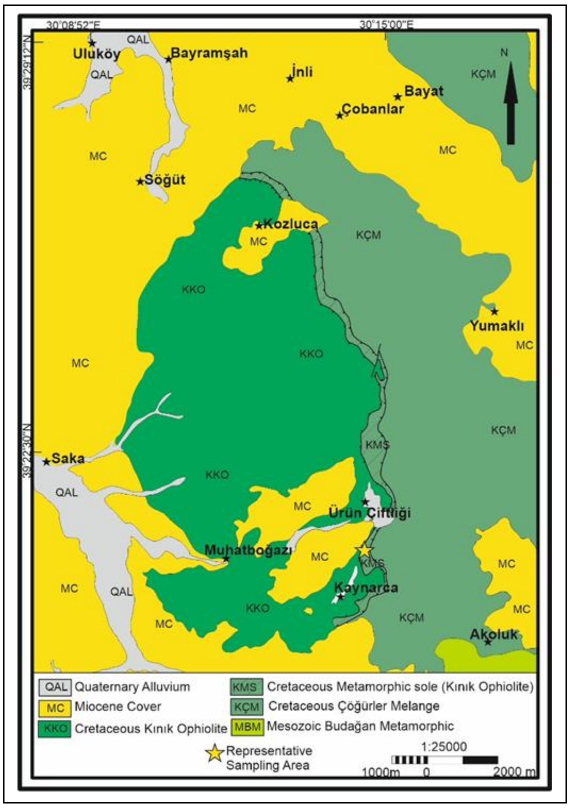

Figure 2. Geological map of the Kaynarca area (IAESZ), showing the main lithological units and their spatial distribution.

The unit shown in yellow as the Miocene Cover north of Kaynarca in Figure 2, although previously interpreted as part of the subophiolitic metamorphic rocks within regional mapping efforts [40], was re-evaluated in this study based on detailed local field observations. These observations indicate that the unit primarily retains sedimentary lithologies and features consistent with the Miocene Cover. Therefore, the classification of this unit as Miocene Cover was preferred in order to reflect the most current and locally verified geological evidence.

Structurally, the metamorphic sole units in the Kaynarca area display the classic inverted metamorphic gradient expected in sub-ophiolitic settings, reflecting the thermal inversion caused by the hot mantle peridotites being thrusted onto cooler crustal material. The structural sequence begins at the base with low-grade schists (amphibolite schists and quartz schists) near the contact with the underlying ophiolitic mélange. The metamorphic grade systematically increases structurally upwards through amphibolites and culminates in high-grade garnet-amphibolites immediately beneath the overlying serpentinites. Garnet-amphibolites occur as layers intercalated with fine-grained amphibolite bands and are characterized by pink garnet crystals intergrown with black, well-crystallized amphiboles. These rocks also show compositional banding of plagioclase and epidote (Figure 3a). The amphibolites are typically brownish-black, strongly foliated, and lack garnet; foliation-parallel banding, albite-epidote veins, and minor faulting are common (Figure 3b).

The upper part of the sequence is dominated by schists, gradually changing from amphibole schists to quartz schists, with occasional quartzite intercalations. Amphibole schists are bluish-green with compositional bands rich in amphibole, plagioclase, and quartz (Figure 3c). Quartz schists are purple-gray in massive exposures and are cut by quartz veins and bands, which emphasize the pervasive deformation affecting these rocks.

3 Analytical techniques

Representative amphibolite samples (n=10) were collected from the subophiolitic metamorphic sequence in the Kaynarca area. Thin sections were prepared and examined under a polarizing microscope to identify mineral assemblages, microstructures, and mineral-mineral relationships. Rim-to-rim pairs of garnet and hornblende were specifically targeted for geothermometric calculations in order to minimize the effects of chemical zoning.

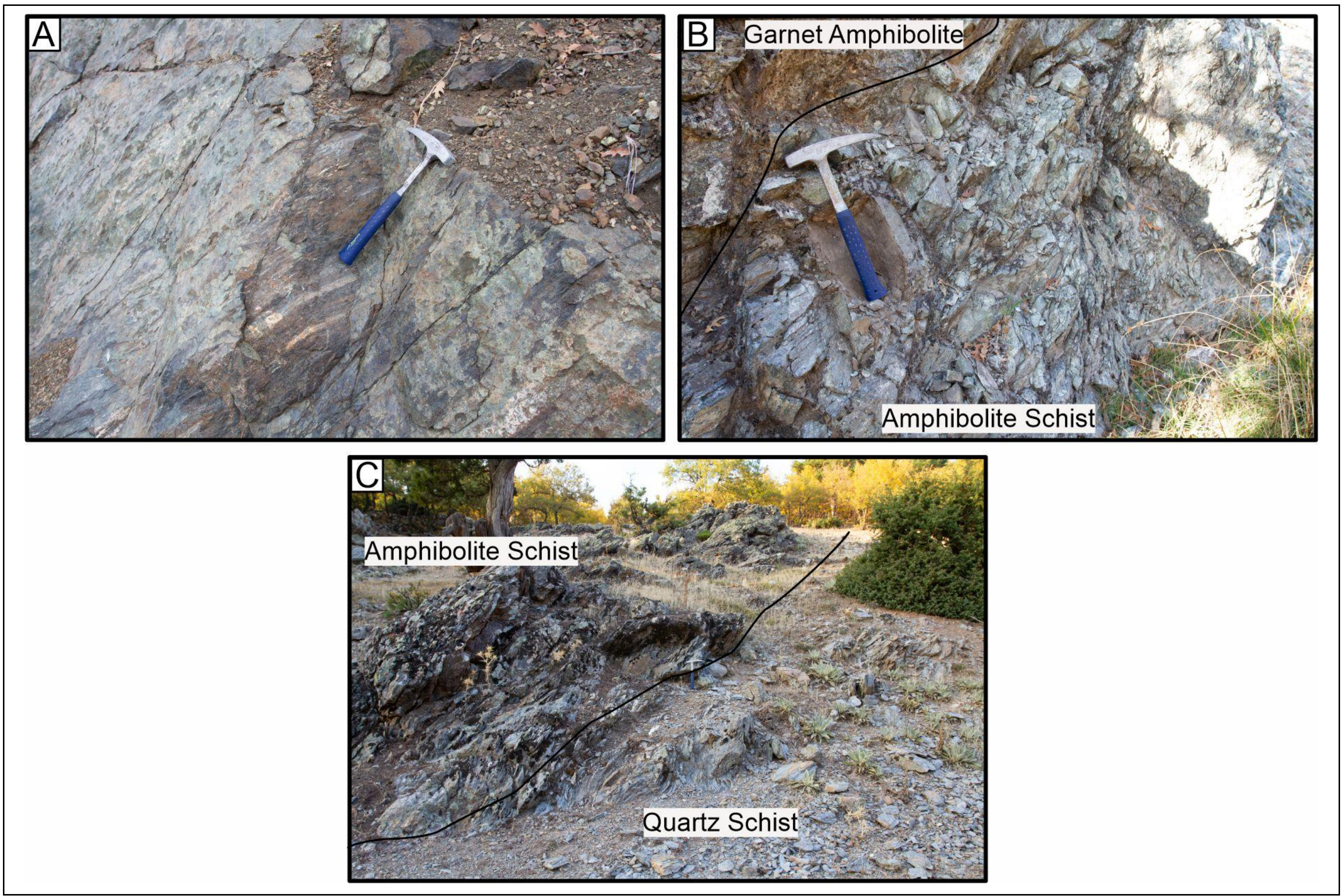

Figure 3. Field photographs of subophiolitic metamorphic rocks from the Kaynarca area (IAESZ). (a): Foliated amphibolite with prominent compositional banding and foliation, indicative of high-temperature deformation. (b): Transition from garnet amphibolite to amphibole schist, marked by pink garnet crystals intergrown with amphibole. (c): Contact between amphibole schist and quartz schist, illustrating the facies change from higher- to lower-grade metamorphism. Black lines mark boundaries between lithological units.

Mineral chemical analyses were carried out at the Central Laboratory (YEBİM), Ankara University, using a JEOL JXA-8230 electron probe micro-analyzer (EPMA). Analytical conditions included an accelerating voltage of 15 kV, a beam current of 15 nA, and a spot size of 1-5 μm. Counting times were typically 10-20 s for major elements and 30-40 s for minor elements. Natural and synthetic mineral standards were used for calibration, and raw data were corrected using a ZAF procedure. A total of two thin sections were analyzed, comprising 21 analytical points on garnet and 32 on amphibole.

We recalculated the cation proportions of amphibole based on 23 oxygen atoms, estimating Fe^{3+}/Fe^{2+} by stoichiometric charge balance [41]. Amphibole structural formula were obtained using the Amphibole P-T Excel spreadsheet [42]. For garnet, cation proportions were recalculated on the basis of 12 oxygen atoms, and end-member components (almandine, pyrope, grossular, spessartine) were determined with the WinGrt program [43]. Amphiboles were classified following the IMA recommendations [44]–[46], whereas garnet nomenclature was based on the IMA garnet supergroup classification [42]. Geothermometry was performed using various garnet–hornblende calibrations [28]–[30], [32], and pressures were evaluated with the Al-in-hornblende barometer [33]. All calculations were performed using modified spreadsheet routines based on published calibrations. Only mineral pairs showing equilibrium values of lnKD ≈ 1.0-1.3 were considered reliable. Analytical uncertainties are estimated at ±30-50 °C for temperature and ±0.5-1 kbar for pressure.

4 Results

4.1 Petrography

Within the metamorphic sole rocks of the Kınık Ophiolite, four principal lithotypes have been distinguished: (i) amphibolite, (ii) garnet-amphibolite, (iii) amphibole schist, and (iv) quartz schist. These units display a variety of metamorphic textures, including granoblastic, nematoblastic, and granonematoblastic fabrics (Figures 4a-d). The sample selected for P-T estimations contains amphibole (35-40 vol.%), garnet (18-20 vol.%), plagioclase (13-15 vol.%), biotite (7-10 vol.%), chlorite (17-20 vol.%), and minor magnetite and titanite (ca. 2 vol.%).

Amphibolites consist mainly of amphibole±plagioclase ±epidote, with subordinate chlorite and opaque Fe-Ti oxides (Figures 4a, b). Quartz inclusions are occasionally observed in amphibole. Garnet-amphibolites contain amphibole+ plagioclase±garnet±biotite±chlorite, with accessory magnetite and titanite. Garnet porphyroblasts commonly reach 1 mm in diameter and are intergrown with black amphibole. Chlorite is secondary and formed during retrogression [47],[48], while plagioclase is strongly altered and lacks polysynthetic twinning.

Amphibole schists are dominated by plagioclase+amphibole ±epidote±titanite and magnetite (Figures 4c, d). They exhibit porphyro-nematoblastic and granoblastic textures, with epidote and amphibole aligned parallel to the foliation. Titanite is generally subhedral. Quartz schists occur as purple-gray, massive layers with quartz veins and bands that emphasize deformation.

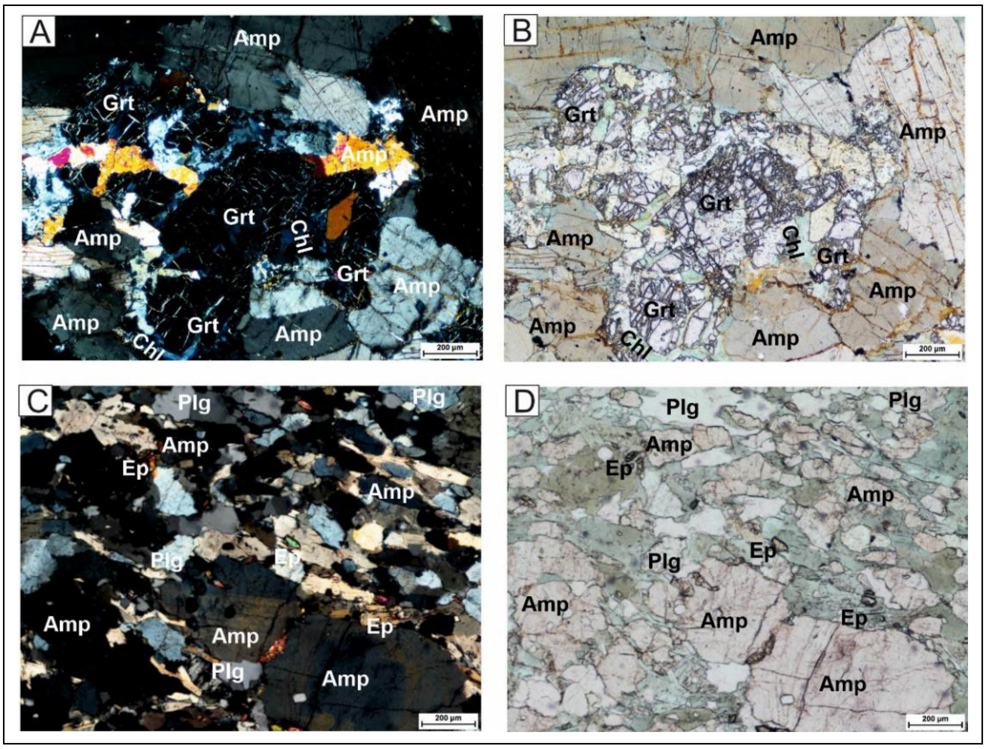

Figure 4. Photomicrographs of representative metamorphic sole rocks from the Kınık Ophiolite (Kaynarca area, IAESZ). (a): Garnet-amphibolite showing garnet (Grt) porphyroblasts intergrown with brown amphibole (Amp) (cross-polarized light). (b): Altered plagioclase (Plg) associated with amphibole (Amp) and secondary epidote (Ep) (plane-polarized light). (c): Amphibolite composed mainly of amphibole and plagioclase with minor opaque phases (cross-polarized light). (d): Amphibole schist with quartz and epidote displaying a foliated texture (plane-polarized light).

Overall, the metamorphic sole sequence shows a progressive change from garnet-bearing amphibolites at the base to amphibole and quartz schist-dominated lithologies upward.

4.2 Mineral chemistry

The mineral chemistry of amphibole and garnet provides critical constraints on the metamorphic conditions and protolith characteristics of the subophiolitic amphibolites. Representative analyses were obtained from carefully selected grains using electron microprobe analysis (Appendix A and Appendix B). Amphibole compositions were recalculated on a 23-oxygen basis, and garnet on a 12-oxygen basis, following IMA recommendations. The results are presented in detail below, together with classification diagrams (Figures 5 and Figure 6), and form the basis for subsequent pressure-temperature estimations.

4.2.1 Garnet

Garnets in the studied subophiolitic amphibolites are dominantly almandine-rich, with significant pyrope and grossular components and only minor spessartine. Average end-member proportions are Alm ~55-65 mol.%, Prp ~15-25 mol.%, Grs ~10-20 mol.%, and Sps generally <5 mol.% (Appendix A). The grains are texturally homogeneous and show no significant compositional zoning between core and rim, suggesting equilibrium growth under stable metamorphic conditions.

In the classification and discrimination diagrams (Figure 5a-d), the analyzed garnets consistently plot within the amphibolite-to granulite-facies domains. The Alm-Prp-Grs ternary diagram shows almandine-dominant compositions [51] (Figure 5a). Figure 5b illustrates that the samples cluster in the amphibolite-granulite transition fields [50], indicating medium- to high-temperature metamorphism. Figure 5c shows that the garnets fall within Type Ci-fields [51], typical of metamorphosed mafic protoliths. Figure 5d shows that the analyzed garnets plot in the basaltic-to-ultrabasic compositional field (<55% pyrope), confirming a mafic protolith origin [52].

These geochemical and mineralogical characteristics collectively suggest crystallization under medium- to high-temperature amphibolite-facies conditions, consistent with subduction-related metamorphism during ophiolite emplacement.

4.2.2 Amphibole

Amphiboles from the subophiolitic amphibolites of the Kınık Ophiolite are dominantly calcic amphiboles, classified mainly as magnesiohornblende and tschermakite, with subordinate ferrohornblende compositions (Figure 6a). This classification is based on the IMA scheme and a recalculated structural formula based on 23 oxygen atoms [44],[46]. The analyzed amphiboles show Mg/(Mg+Fe^{2+}) ratios between 0.45 and 0.65, reflecting intermediate Fe-Mg compositions typical of amphibolite-facies assemblages.

Further discrimination of amphibole compositions was carried out using the Ca+Na+K versus Si (apfu) diagram of [53] (Figure 6b). In this projection, most amphibole analyses fall within the magmatic field, although some data points trend toward the metamorphic domain.

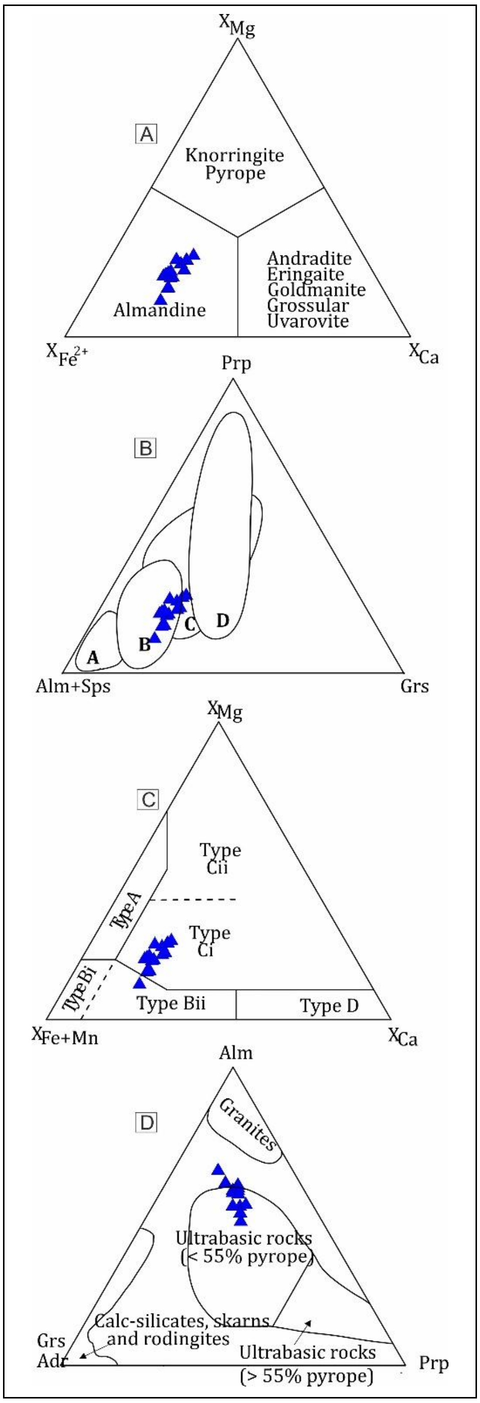

Figure 5. Classification and discrimination diagrams of garnets from the subophiolitic amphibolites of the Kınık Ophiolite. (a): Alm-Prp-Grs ternary diagram showing almandine-dominated compositions [49]. (b): Provenance discrimination fields showing that the garnets plot within the amphibolite-granulite transition domains [50]. (c): Classification fields indicating that the analyzed garnets fall within Type Ci fields typical of metamorphosed mafic rocks [51]. (d): Ternary compositional diagram demonstrating that the analyzed garnets plot in the basaltic to ultrabasic compositional fields (< 55% pyrope), confirming a mafic protolith affinity [52].

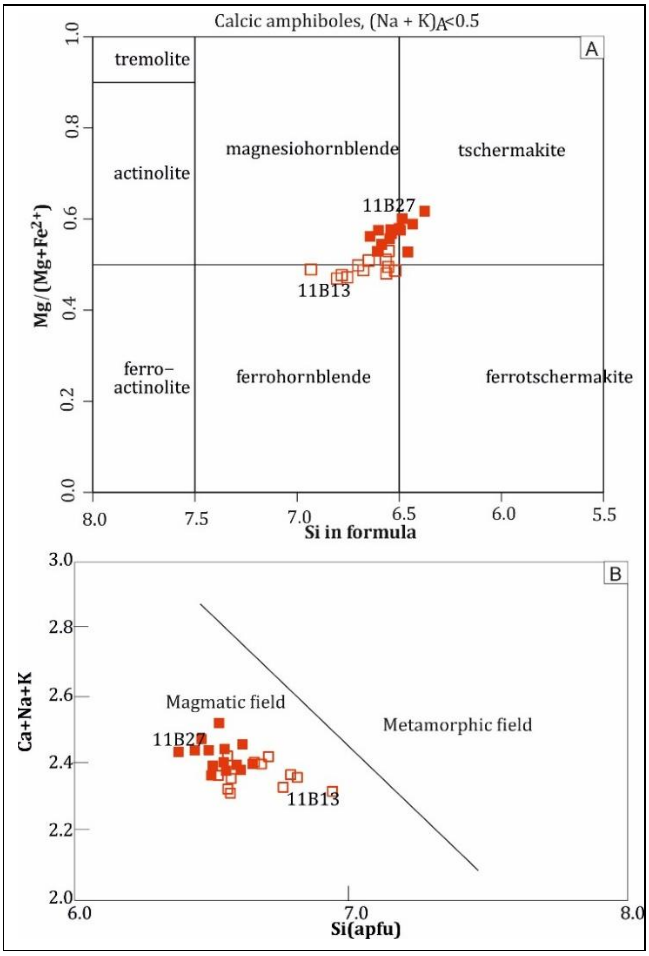

Figure 6. Classification and discrimination diagrams of amphiboles from the subophiolitic amphibolites of the Kınık Ophiolite. (a): IMA classification plot showing amphiboles mainly in the fields of magnesiohornblende and tschermakite. (b): Ca+Na+K versus Si (apfu) diagram (after [53]), indicating that most amphiboles retain magmatic affinities with partial metamorphic re-equilibration.

4.3 Pressure-Temperature calculation

Geothermometric estimations based on garnet-hornblende pairs provide quantitative constraints on the peak metamorphic conditions of the studied amphibolites. In this study, we applied several calibrations [28]-[30],[32]. These thermometers rely on Fe-Mg exchange between garnet and hornblende. The garnet-hornblende thermometry and Al-in-hornblende barometry results are summarized in Table 1. Only mineral pairs fulfilling equilibrium criteria were considered: amphibole structural formula were calculated on a 23 O basis with Fe^{3+}/Fe^{2+} partitioning after [36], garnet end-member proportions (XFe, XMg, XMn, XCa) were constrained to sum ≈1. Furthermore, only analyses with lnKD values between 1.0 and 1.3 were included [29],[30].

Multiple analyses were obtained from two representative samples: 11B13 (n = 14) and 11B27 (n = 7). In sample 11B13, calculated temperatures range from ~708 to ~804 °C, depending on the calibration, with an average of ~740 °C. These values indicate metamorphism under upper amphibolite-facies conditions, locally approaching the granulite-facies transition. In sample 11B27, temperatures range from ~671 to 729 °C, with an average of ~700 °C. These results correspond to medium amphibolite facies conditions.

We estimated pressures using the Al-in-hornblende barometer [33]. This method is based on the total Al content of hornblende and does not require a plagioclase pair. The results are as follows:

- For 11B13 (n = 14), the mean pressure is ~5.2 kbar, equivalent to a depth of ~19 km (assuming a crustal density of 2.7 g/cm^3).
- For 11B27 (n = 7), the mean pressure is ~3.9 kbar, corresponding to a depth of ~14.5 km.

Taken together, the garnet-hornblende thermometers and the Al-in-hornblende barometer indicate that the studied amphibolites equilibrated at ~640-790 °C and ~4-5 kbar, corresponding to medium- to upper-amphibolite facies conditions. Notably, the relatively higher temperatures in sample 11B13, within the same pressure range, suggest a low-pressure/high-temperature (LP-HT) metamorphic regime. These findings demonstrate that the subophiolitic metamorphic sole rocks developed at mid-crustal depths (~14-20 km) during tectonic emplacement of the Kınık Ophiolite.

Table 1. P-T estimates for amphibolite samples 11B13 and 11B27 from the Kınık Ophiolite, based on garnet-hornblende thermometry and Al-in-hornblende barometry.

Sample	[28]			[29]			[30]			[32]		[33]	D (kbar≈3.7 km)
	lnKD	T(K)	T(c)	lnKD	T(K)	T(c)	lnKD	T(K)	T(c)	T	T(c)	P (±0.5kbar) =3.46+4.23 Al	
11B13 (n14)	1.0826	1017.7	744.7	1.0826	981.7	708.7	1.0826	1076.9	803.9	727.5	668	5.24	19.38
11B27 (n7)	1.2163	993.5	720.5	1.2163	944	671	1.2163	1002	729	702.6	656.9	3.92	14.49

5 Discussions

The detailed field observations and analytical data obtained from the well-preserved metamorphic sequence in the Kaynarca area provide valuable evidence for subduction-related metamorphism and the tectonic emplacement of ophiolitic complexes within the İzmir-Ankara-Erzincan Suture Zone (İAESZ). These findings contribute to a broader understanding of the tectonic evolution of the Neotethyan oceanic lithosphere. The petrographic characteristics emphasize the structural position of the metamorphic sole and its formation under high-temperature, subduction-related metamorphic conditions. Garnet porphyroblasts in the garnet-amphibolites indicate growth under peak amphibolite-facies conditions and serve as reliable phases for geothermometric calculations [2],[14],[37],[38]. Strong foliation in amphibolites and amphibole schists, together with quartz veining in quartz schists, documents deformation associated with subduction-driven tectonism [14].

Garnet compositions indicate crystallization under medium- to upper-amphibolite-facies conditions, suggesting basaltic protoliths with MORB- to OIB-like affinities. Amphibole compositions are likewise consistent with crystallization within the medium-to upper-amphibolite-facies field, in agreement with garnet compositions and P-T estimates derived from geothermobarometry. The intermediate Fe-Mg character and Al_{tot} contents of amphiboles provide robust constraints on metamorphic pressures of approximately 4-5 kbar. The geochemical features further suggest that the amphiboles retain partial magmatic signatures, subsequently modified under metamorphic conditions during intra-oceanic subduction, as reported for other metamorphic soles. Chlorite occurs as a retrograde phase formed during cooling and decompression, consistent with greenschist facies assemblages previously described from the Kaynarca area [14].

P-T calculations confirm that the Kınık amphibolites record peak conditions of 640-790 °C and 4-5 kbar, defining a High-Temperature/Low-Pressure (HT/LP) regime consistent with the regional model of inverted metamorphism during intra-oceanic thrusting. However, unlike earlier studies on the same Kaynarca sole complex [14], [40], which reported a subsequent High-Pressure/Low-Temperature (HP/LT) overprint characterized by partial replacement of calcic amphiboles by sodic (Na-rich) amphiboles, our data do not reveal evidence of such a secondary metamorphic phase. Amphiboles in our samples consistently display stable calcic compositions (magnesiohornblende to tschermakite) typical of the HT/LP metamorphic event, with no significant development of sodic amphiboles.

The absence of this HP/LT overprint in our dataset indicates a spatial heterogeneity within the Kaynarca sole complex. The HP/LT effects may be restricted to localized tectonic slices that were briefly subducted to greater depths, or, alternatively, the analyzed section may have experienced a rapid exhumation path that limited or erased the HP imprint before cooling under greenschist-facies conditions. Consequently, this study documents a segment of the Kaynarca metamorphic sole that preserves pure HT/LP peak conditions followed by limited retrogression, providing refined constraints on the variability and extent of metamorphic overprinting within the İAESZ ophiolite complexes.

These results underscore the heterogeneous nature of subophiolitic metamorphic soles along the İzmir-Ankara-Erzincan Suture Zone (İAESZ). The mineralogical and thermobarometric data from the Kaynarca segment reveal that not all sections of the metamorphic sole experienced the same degree of metamorphic overprinting. Instead, variations in the preservation of HT/LP and HP/LT imprints likely reflect localized differences in subduction depth, thermal gradients, and exhumation rates. Therefore, the Kaynarca metamorphic sole provides an important example of how subduction-related metamorphism can exhibit significant spatial variability, even within a single ophiolitic complex, offering refined insights into the dynamics of intra-oceanic subduction and ophiolite emplacement.

6 Conclusion

The subophiolitic metamorphic sole of the Kınık Ophiolite provides significant insights into the metamorphic and tectonic evolution of the İzmir-Ankara-Erzincan Suture Zone. Petrographic observations reveal that the sole sequence is dominated by amphibolites, garnet-amphibolites, amphibole schists, and quartz schists, which record medium- to high-temperature mineral assemblages subsequently overprinted by retrograde phases such as chlorite and epidote.

Mineral chemistry of garnet and amphibole further constrains the metamorphic evolution. Garnets are almandine-rich with subordinate pyrope and grossular and negligible spessartine, plotting within the amphibolite-granulite facies fields of discrimination diagrams. Amphiboles are predominantly calcic types, classified as magnesiohornblende and tschermakite, with compositions that partly preserve magmatic signatures but also reflect metamorphic re-equilibration.

Geothermobarometric calculations based on garnet-hornblende thermometry and the Al-in-hornblende barometer indicate peak metamorphic conditions of ~640-790 °C and ~4-5 kbar, corresponding to medium- to upper-amphibolite facies. These values imply equilibration at mid-crustal depths (~14-20 km). The relatively higher temperatures recorded in sample 11B13 indicate a low-pressure/high-temperature (LP-HT) metamorphic regime, typical of metamorphic soles formed during intra-oceanic subduction and subsequent ophiolite emplacement. Overall, the integrated petrographic, mineral chemical, and geothermobarometric data demonstrate that the subophiolitic amphibolites of the Kınık Ophiolite formed from basaltic protoliths with MORB- to OIB-like affinities [14] and were metamorphosed under LP-HT conditions during the tectonic emplacement of the ophiolite.

7 Acknowledgments

This study is based on data that were also presented at the 10th Geochemistry Symposium under the title "Origin and Age of the Metamorphic Sole Rocks of the Kınık Ophiolite (Kütahya)" The research was financially supported by the Scientific Research Projects Coordination Unit of Kütahya Dumlupınar University (Project No: 2021-11). The author would like to thank Prof. Dr. Osman Parlak, Prof. Dr. Utku Bağcı, and Dr. Emrah Şimşek once again for their continuous scientific guidance, constructive comments, and collaboration throughout this research.

The author also extends sincere gratitude to all colleagues and institutions that provided logistical and technical support during the field and laboratory stages of this study.

Finally, the author gratefully acknowledges the constructive comments and valuable suggestions provided by the anonymous reviewers, which significantly improved the quality of the manuscript, as well as the handling editor for their careful evaluation and guidance throughout the review process.

8 Author contribution statements

In the scope of this study, İrem Aksoy contributed to the conceptualization, field investigation, data collection, formal analysis, visualization, and writing of the original draft. The author also designed the methodology and interpreted the results.

9 Ethics committee approval and conflict of interest statement

"Ethics committee approval was not required for the preparation of this article". "The authors declare no conflict of interest with any individual or institution in relation to the preparation of this article".

10 References

[1] Moores EM. "Origin and emplacement of ophiolites". Reviews of Geophysics, 20(4), 735-60, 1982.

[2] Okay AI, Tuysuz O. "Tethyan sutures of northern Turkey". Geological Society, London, Special Publications, 156, 475-515, 1999.

[3] Dilek Y, Furnes H. "Ophiolites and their origins". Elements. 10(2), 93-100, 2014.

[4] Wakabayashi J, Dilek Y. "What constitutes 'emplacement' of an ophiolite?: Mechanisms and relationship to subduction initiation and formation of metamorphic soles". Geological Society, London, Special Publications. 218(1), 427-447, 2008.

[5] Çelik ÖF, Delaloye MF. "Characteristics of ophiolite-related metamorphic rocks in the Beysehir ophiolitic mélange (Central Taurides, Turkey), deduced from whole rock and mineral chemistry". Journal of Asian Earth Sciences, 26(5), 461-76, 2006.

[6] Önen AP, Hall R. Sub-ophiolite metamorphic rocks from NW Anatolia, Turkey. Journal of Metamorphic Geology. 18(5), 483-95, 2000.

[7] Kotowski AJ, Cloos M, Stockli DF, Bos Orent E. "Structural and Thermal Evolution of an Infant Subduction Shear Zone: Insights From Sub-Ophiolite Metamorphic Rocks Recovered From Oman Drilling Project Site BT-1B". Journal of Geophysical Research: Solid Earth, 126(12), e2021JB021702, 2021

[8] Rioux M, Garber J, Bauer A, Bowring S, Searle M, Kelemen P, et al. "Synchronous formation of the metamorphic sole and igneous crust of the Semail ophiolite: New constraints on the tectonic evolution during ophiolite formation from high-precision U-Pb zircon geochronology". Earth and Planetary Science Letters, 451, 185-95, 2016.

[9] Searle MP, Waters DJ, Martin HN, Rex DC. "Structure and metamorphism of blueschist-eclogite facies rocks from the northeastern Oman Mountains". Journal of the Geological Society, 151(3), 555-576, 1994.

[10] Searle MP, Malpas J. "Petrochemistry and origin of sub-ophiolitic metamorphic and related rocks in the Oman Mountains". Journal of the Geological Society, 139(3), 235-48, 1982.

[11] Gnos E, Peters T. "K-Ar ages of the metamorphic sole of the Semail Ophiolite: implications for ophiolite cooling history". Contributions to Mineralogy and Petrology, 113(3), 325-32, 1993.

[12] Çelik ÖF. "Metamorphic sole rocks and their mafic dykes in the eastern Tauride belt ophiolites (southern Turkey): Implications for OIB-type magma generation following slab break-off". Geological Magazine, 144(5), 849-66, 2007.

[13] Dilek Y, Whitney DL. "Counterclockwise P-T-t trajectory from the metamorphic sole of a Neo-Tethyan ophiolite (Turkey)". Tectonophysics, 280(3-4), 295-310, 1997.

[14] Önen AP, Hall R. "Ophiolites and related metamorphic rocks from the Kütahya region, north-west Turkey". Geological Journal, 28(3-4), 399-412, 1993.

[15] Çelik ÖF. "Detailed geochemistry and K-Ar geochronology of the metamorphic sole rocks and their mafic dykes from the Mersin ophiolite, southern Turkey". Turkish Journal of Earth Sciences, 17(4),685-708, 2008.

[16] Çelik ÖF, Delaloye MF. "Origin of metamorphic soles and their post-kinematic mafic dyke swarms in the Antalya and Lycian ophiolites, SW Turkey". Geological Journal, 38(3-4), 235-56, 2003.

[17] Çelik ÖF, Delaloye MF. "Characteristics of ophiolite-related metamorphic rocks in the Beyşehir ophiolitic mélange (Central Taurides, Turkey), deduced from whole rock and mineral chemistry". Journal of Asian Earth Science, 26(5), 461-76, 2006.

[18] Parlak O, Delaloye M, Bingöl E. "Origin of sub-ophiolitic metamorphic rocks beneath the Mersín ophiolite, southern Turkey". Ofioliti, 20(2), 97-110, 1995.

[19] Vergili Ö, Parlak O. "Geochemistry and tectonic setting of metamorphic sole rocks and mafic dikes from the pinarbaşi (Kayseri) ophiolite, Central Anatolia (Turkey)". Ofioliti, 30(1), 37-52, 2005.

[20] Parlak O, Yilmaz H, Boztuğ D. "Origin and tectonic significance of the metamorphic sole and isolated dykes of the Divriği ophiolite (Sivas, Turkey): Evidence for slab break-off prior to ophiolite emplacement". Turkish Journal of Earth Sciences, 15(1), 25-45, 2006.

[21] Dilek Y, Thy P. "Structure, petrology and seafloor spreading tectonics of the Kizildag Ophiolite, Turkey". Geological Society, London, Special Publications, 148, 43-69, 1998.

[22] Robertson AHF. "Overview of the genesis and emplacement of Mesozoic ophiolites in the Eastern Mediterranean Tethyan region". Lithos, 65(1-2), 1-67, 2002.

[23] Sarıfakıoğlu E, Sevin M, Dilek Y. "Türkiye Ofiyolitleri. Özel Yayın Serisi-35 MTA, 2017.

[24] Çörtük RM, Çelik ÖF, Özkan M, Sherlock SC, Marzoli A, Altıntaş İE, Topuz G. "Origin and geodynamic environments of the metamorphic sole rocks from the İzmir-Ankara-Erzincan suture zone (Tokat, northern Turkey)". International Geology Review, 58(15), 1839-1855, 2016.

[25] Üner T, Çakır Ü. "A deformation structure and origin of metamorphic sole rocks beneath the Eldivan and Ahlat ophiolites (Çankırı), Northern Anatolia". Journal of Scientific Reports-A, 62, 90-110, 2025.
[26] Özbey Z, Ustaömer T, Robertson AH, Ustaömer PA. "Tectonic significance of Late Ordovician granitic magmatism and clastic sedimentation on the northern margin of Gondwana (Tavşanlı Zone, NW Turkey)". Journal of the Geological Society, 170(1), 159-173, 2013.
[27] Plunder A, Agard P, Chopin C, Okay AI. "Geodynamics of the Tavşanlı zone, western Turkey: Insights into subduction/obduction processes". Tectonophysics, 608, 884-903, 2013.
[28] Graham CM, Powell RA. "Garnet-hornblende geothermometer: calibration, testing, and application to the Pelona Schist, Southern California". Journal of Metamorphic Geology, 2(1), 13-31, 1984.
[29] Perchuk LI, Aranovıch LY, Podlesskıı KK, Lavrant'eva I V. Gerasımov VY, Fed'kın V V. "Precambrian granulites of the Aldan shield, eastern Siberia, USSR". Journal of Metamorphic Geology, 3(3), 265-310, 1985.
[30] Ravna EK. "Distribution of Fe2+ and Mg between coexisting garnet and hornblende in synthetic and natural systems: an empirical calibration of the garnet-hornblende Fe-Mg geothermometer". Lithos, 53(3-4), 265-77, 2000.
[31] Thomas H, Rana H. "Garnet-Hornblende Geothermometer: A Comparative Study". Journal of the Geological Society of India, 96(6), 591-6, 2020.
[32] Powell R. "Regression diagnostics and robust regression in geothermometer/geobarometer calibration: the garnet-clinopyroxene geothermometer revisited". Journal of Metamorphic Geology, 3(3), 231-43, 1985.
[33] Johnson MC, Rutherford MJ. "Experimental calibration of the aluminium-in-hornblende geobarometer with application to long valley caldera (California) volcanic rock". Geology, 17(9), 837-841, 1989.
[34] Dilek Y, Moores EM, Delaloye M, Karson JA. "Amagmatic extension and tectonic denudation in the Kizildağ Ophiolite, Southern Turkey: Implications for the evolution of Neotethyan oceanic crust". In Ophiolite Genesis and Evolution of the Oceanic Lithosphere: Proceedings of the Ophiolite Conference, Muscat, Oman, 7-18 January 1990.
[35] Robertson AHF. "Role of the tectonic facies concept in orogenic analysis and its application to Tethys in the Eastern Mediterranean region". Earth-Science Reviews, 37(3-4), 139-213, 1994.
[36] Dilek Y, Furnes H. "Structure and geochemistry of Tethyan ophiolites and their petrogenesis in subduction rollback systems". Lithos, 113(1-2), 1-20, 2009.
[37] Uysal I, Tarkian M. "Petrogenesis of the ophiolitic chromitites from Mugla-Isparta-Antalya areas (SW-Turkey): Platinum-Group Minerals and Mafic Silicate Inclusions in Chromite". 10th Int Platinum Symp (Oulu),. University of Oulu, Oulu, 2005.
[38] Şengör AC, Yilmaz Y. "Tethyan evolution of Turkey: a plate tectonic approach". Tectonophysics, 75(3-4), 181-241, 1981.
[39] Özcan A, Göncüoğlu MC, Turhan N, Uysal S, Şentürk K, Işık A. "Late Paleozoic evolution of the Kütahya-Bolkardağ belt". METU Journal of Pure and Applied Science, 21(1/3), 211-20, 1988.
[40] Göncüoğlu MC. "Kütahya-Bolkardağ Kuşağının Jeolojisi". MTA Dergisi, 142, 227-82, 2011.
[41] Schumacher JC. "The estimation of ferric iron in electron microprobe analysis of amphiboles". Mineralogical Magazine, 61(405), 312-21, 1997.
[42] Putirka KD. "Thermometers and barometers for volcanic systems". Reviews in mineralogy and geochemistry, 69(1), 61-120, 2008.
[43] Yavuz F, Kıran Yıldırım D. "WinGrt, a Windows program for garnet supergroup minerals". Journal of Geosciences, 65, 71-95, 2020.
[44] Leake BE. "Nomenclature of amphiboles. Mineralogical Magazine, 61, 296-311, 1997.
[45] Leake BE, Woolley AR., Birch WD, Burke EA, Ferraris G, Grice JD, Whittaker EJ. "Nomenclature of amphiboles: additions and revisions to the International Mineralogical Association's 1997 recommendations". The Canadian Mineralogist, 41(6), 1355-1362, 2003.
[46] Hawthorne FC, Oberti R, Harlow GE, Maresch WV, Martin RF, Schumacher JC, et al. "Nomenclature of the amphibole supergroup". American Mineralogist, 97(11-12), 2031-48, 2012.
[47] Bucher K, Grapes R. Metamorphic rocks. In Petrogenesis of Metamorphic Rocks. Berlin, Heidelberg, Springer, 2011.
[48] Spear FS. Metamorphic Phase Equilibria And Pressure-Temperature-Time Paths. Mineralogical Society of America Monograph., 352, 1993.
[49] Grew ES, Locock AJ, Mills SJ, Galuskina IO, Galuskin E V., Hålenius U. "Nomenclature of the garnet supergroup". American Mineralogist, 98(4), 785-811, 2013.
[50] Mange MA, Morton AC. "Geochemistry of heavy minerals". Developments in Sedimentology, 58, 345-91, 2007.
[51] Aubrecht R, Meres S, Sýkora M, Mikus T. "Provenance of the detrital garnets and spinels from the Albian sediments of the Czorsztyn Unit (Pieniny Klippen Belt, Western Carpathians, Slovakia)". Geologica Carpathica, 60(6), 463, 2009.
[52] Suggate SM, Hall R. Using Detrital Garnet Compositions to Determine Provenance: A New Compositional Database And Procedure, Editors: R. A. Scott, H. R. Smyth, A. C. Morton, N. Richardson. Sediment Provenance Studies in Hydrocarbon Exploration and Production, Geological Society, London, Special Publications, 373-393. 2014.
[53] Giret A, Bonin B, Leger JM. "Amphibole compositional trends in oversaturated and undersaturated alkaline plutonic ring-complexes". The Canadian Mineralogist, 18, 481-495, 1980.

Appendix A.

Representative electron microprobe analyses of garnet from subophiolitic amphibolites of the Kınık Ophiolite (mol. % end-member proportions: Alm, Prp, Grs, Sps).

	11B13											11B27									
Point No	1	2	5	6	7	8	9	10	11	13	14	15a	15b	16	17	18	19	20	21	22	23
MgO	5.11	5.154	5.272	4.094	5.68	3.905	4.442	5.398	4.398	5.276	5.297	6.106	6.405	6.258	6.301	6.342	6.036	6.031	6.079	5.934	6.375
SiO_2	38.42	39.27	36.01	36.84	38.87	36.46	39.04	39.49	35.41	40.89	43.34	33.95	39.92	40.13	41.59	40.95	41.2	41.32	41.33	41.33	40.82
Na_2O	0.047	0.063	0.021	0.044	0.055	0.026	0	0.031	0.037	0.016	0.053	0.024	0.017	0.007	0	0.058	0.044	0.009	0.062	0.014	0.029
Al_2O_3	21.82	22.27	20.86	21.06	21.87	21.69	21.6	21.57	20.92	21.56	21.79	22.17	21.94	22.2	22.11	21.87	21.67	22	21.91	21.8	22.08
MnO	0.492	1.25	0.515	1.394	0.682	1.524	0.759	0.645	0.912	1.307	1.295	1.027	0.994	1.007	0.803	0.99	0.977	0.752	0.653	0.626	0.73
FeO	26.84	24.89	29.87	28.7	26.05	28.35	26.62	25.76	30.42	23.97	21.3	28.21	23.09	22.38	21.72	21.85	22	21.62	21.68	21.62	21.72
TiO_2	0.122	0.17	0.121	0.183	0.066	0.086	0.129	0.103	0.099	0.026	0.185	0.227	0.252	0.107	0.11	0.276	0.35	0.14	0.188	0.346	0.203
Cr_2O_3	0.004	0	0.003	0.004	0.011	0.009	0.002	0	0.015	0.015	0.032	0.017	0.002	0.01	0	0.002	0	0.012	0	0.025	0
K_2O	0.007	0.002	0	0	0.003	0	0	0.004	0.003	0.04	0.007	0.006	0.006	0.006	0.006	0.003	0.005	0.004	0	0.006	0.003
CaO	7.431	6.56	7.049	7.189	6.587	7.345	7.62	6.351	7.598	6.362	7.175	7.374	7.156	6.923	7.182	7.151	7.328	7.369	7.403	7.803	7.498
Total	100.3	99.63	99.73	99.52	99.87	99.39	100.2	99.35	99.81	99.46	100.5	99.11	99.78	99.03	99.83	99.5	99.61	99.26	99.3	99.5	99.46
Si	2.992	3.044	2.861	2.933	3.02	2.909	3.038	3.07	2.831	3.143	3.24	2.715	3.063	3.087	3.149	3.122	3.137	3.149	3.148	3.144	3.113
Ti	0.007	0.01	0.007	0.011	0.004	0.005	0.008	0.006	0.006	0.002	0.01	0.014	0.015	0.006	0.006	0.016	0.02	0.008	0.011	0.02	0.012
Al	2.003	2.034	1.953	1.976	2.003	2.04	1.98	1.976	1.971	1.953	1.92	2.089	1.983	2.012	1.972	1.965	1.945	1.976	1.967	1.954	1.985
Cr	0	0	0	0	0.001	0.001	0	0	0.001	0.001	0.002	0.001	0	0.001	0	0	0	0.001	0	0.002	0
$Fe^{(III)}$	0	0	0.179	0.079	0	0.046	0.012	0.018	0.191	0.045	0.068	0.181	0.002	0	0.022	0.019	0.035	0.016	0.023	0.025	0.004
Mg	0.593	0.596	0.624	0.486	0.658	0.464	0.515	0.626	0.524	0.605	0.59	0.728	0.733	0.718	0.711	0.721	0.685	0.685	0.69	0.673	0.725
Ca	0.62	0.545	0.6	0.613	0.548	0.628	0.635	0.529	0.651	0.524	0.575	0.632	0.588	0.571	0.582	0.584	0.598	0.602	0.604	0.636	0.613
Mn	0.032	0.082	0.035	0.094	0.045	0.103	0.05	0.042	0.062	0.085	0.082	0.07	0.065	0.066	0.051	0.064	0.063	0.049	0.042	0.04	0.047
$Fe^{(II)}$	1.748	1.613	1.806	1.831	1.692	1.846	1.72	1.657	1.842	1.496	1.264	1.705	1.48	1.44	1.354	1.375	1.366	1.362	1.358	1.351	1.381
Na	0.007	0.009	0.003	0.007	0.008	0.004	0	0.005	0.006	0.002	0.008	0.004	0.003	0.001	0	0.009	0.006	0.001	0.009	0.002	0.004
Cat. Tot.	8.002	7.933	8.068	8.03	7.979	8.046	7.958	7.929	8.085	7.856	7.759	8.139	7.932	7.902	7.847	7.875	7.855	7.849	7.852	7.847	7.884
Prp	19.77	20.93	20.35	16.03	22.29	15.25	17.64	21.88	16.99	22.29	23.44	23.2	25.55	25.68	26.35	26.19	25.21	25.39	25.53	24.91	26.17
Grs	20.66	19.15	17.81	19.42	18.57	20.15	21.62	18.34	19.08	18.88	22.04	18.31	20.49	20.42	21.35	21.02	21.61	22.12	22.09	23.25	22.07
Sps	1.08	2.88	1.13	3.1	1.52	3.38	1.71	1.49	2	3.14	3.26	2.22	2.25	2.35	1.91	2.32	2.32	1.8	1.56	1.49	1.7
Alm	58.25	56.7	58.86	60.42	57.34	60.61	58.89	57.97	59.72	55.16	50.18	54.33	51.6	51.52	50.16	49.95	50.24	50.47	50.23	49.99	49.86
Alm+Sps	59.33	59.58	59.99	63.52	58.86	63.99	60.6	59.46	61.72	58.3	53.44	56.55	53.85	53.87	52.07	52.27	52.56	52.27	51.79	51.48	51.56

Appendix B.

Representative electron microprobe analyses of amphibole from subophiolitic amphibolites of the Kınık Ophiolite (structural formulae calculated on the basis of 23 oxygens).

	11B13												1B27																			
	1a	1b	2a	2b	3a	3b	4a	4b	5a	5b	6a	6b	7a	7b	8a	8b	9a	9b	10a	10b	11a	11b	12	13	14	15	16	17	18	19	20	23
Na_2O	2.1	2.0	2.2	2.3	2.5	2.5	2.2	2.3	2.4	2.2	2.2	2.3	1.8	1.6	2.2	1.4	2.3	2.2	2.2	1.5	1.7	1.4	2.3	1.4	2.1	1.6	2.3	2.2	2.3	1.6	2.3	2.2
MgO	8.3	8.7	8.3	8.6	8.6	9.1	9.0	8.9	8.5	8.0	8.0	8.0	8.1	8.5	10.2	9.4	9.5	9.5	9.5	9.4	9.7	9.5	9.2	9.3	9.6	9.6	10.1	10.3	10.3	9.5	9.8	9.9
Al_2O_3	12.6	11.5	12.4	12.7	13.0	13.3	12.6	12.9	12.7	13.8	13.2	13.1	5.5	4.7	14.0	6.6	14.4	14.5	13.8	6.8	6.4	6.1	14.3	6.4	13.4	6.7	14.3	14.5	14.0	5.7	14.1	13.8
MnO	0.0	0.0	0.0	0.0	0.0	0.0	0.0	0.0	0.0	0.0	0.0	0.0	0.0	0.0	0.0	0.0	0.0	0.0	0.0	0.0	0.0	0.0	0.0	0.0	0.0	0.0	0.0	0.0	0.0	0.0	0.0	0.0
SiO_2	45.6	46.8	46.2	46.6	45.6	44.3	45.0	45.7	44.1	44.5	43.7	43.3	50.4	51.9	45.7	52.3	45.4	44.5	44.0	51.3	52.3	52.4	44.0	52.0	45.3	45.7	43.9	43.3	44.2	52.1	44.3	45.0
K_2O	0.6	0.6	0.5	0.5	0.5	0.5	0.5	0.5	0.6	0.6	0.6	0.6	0.0	0.0	0.4	0.0	0.4	0.4	0.4	0.0	0.0	0.0	0.4	0.0	0.4	0.0	0.5	0.5	0.4	0.0	0.5	0.5
FeO	16.6	16.1	16.7	16.8	16.6	16.1	16.6	15.9	17.2	17.0	16.9	17.2	11.5	10.9	13.9	9.4	14.4	14.1	15.5	9.5	9.2	9.6	15.8	9.6	15.5	9.7	14.3	14.1	14.0	9.5	14.3	14.9
TiO_2	1.5	1.4	1.4	1.3	1.5	1.4	1.2	1.6	1.7	1.7	1.7	1.7	0.5	0.4	1.3	0.5	1.3	1.2	1.0	0.4	0.4	0.4	1.0	0.4	1.0	0.3	1.3	1.1	1.1	0.4	1.3	1.2
Cr_2O_3	0.0	0.0	0.0	0.0	0.0	0.0	0.0	0.0	0.0	0.0	0.0	0.0	0.0	0.0	0.0	0.0	0.0	0.0	0.0	0.0	0.0	0.0	0.0	0.0	0.0	0.0	0.0	0.0	0.0	0.0	0.0	0.0
CaO	10.2	10.4	10.3	10.4	10.2	10.3	10.6	10.7	9.8	10.0	9.7	9.8	21.6	21.1	10.9	20.1	10.7	10.7	10.6	20.2	20.3	20.5	11.2	20.4	11.4	20.0	10.9	10.8	10.8	20.3	10.5	10.9
Total	97.4	97.5	98.1	99.1	98.6	97.4	97.8	98.5	97.0	97.8	96.0	96.0	99.3	99.1	98.6	99.7	98.6	97.0	97.0	99.1	99.9	99.9	98.1	99.5	98.8	93.5	97.6	96.8	97.2	99.2	97.2	98.6
Si	6.8	6.9	6.8	6.8	6.7	6.6	6.7	6.7	6.6	6.6	6.6	6.5	8.3	8.5	6.6	8.3	6.6	6.5	6.5	8.2	8.3	8.3	6.5	8.3	6.6	7.8	6.4	6.4	6.5	8.3	6.5	6.5
$Al^{(IV)}$	1.2	1.1	1.2	1.2	1.3	1.4	1.4	1.3	1.4	1.4	1.4	1.5	0.0	0.0	1.4	0.0	1.4	1.5	1.5	0.0	0.0	0.0	1.5	0.0	1.4	0.2	1.6	1.6	1.5	0.0	1.5	1.5
$Al^{(VI)}$	0.9	0.9	1.0	1.0	0.9	0.9	0.8	0.9	0.8	1.0	0.9	0.9	1.1	0.9	1.0	1.2	1.0	1.1	0.9	1.3	1.2	1.1	0.9	1.2	0.9	1.1	0.9	0.9	0.9	1.1	0.9	0.9
$Fe^{(III)}$	0.0	0.0	0.0	0.0	0.1	0.2	0.2	0.0	0.3	0.2	0.3	0.3	0.0	0.0	0.1	0.0	0.0	0.1	0.4	0.0	0.0	0.0	0.1	0.0	0.0	0.0	0.2	0.3	0.2	0.0	0.2	0.2
Ti	0.2	0.2	0.2	0.1	0.2	0.2	0.1	0.2	0.2	0.2	0.2	0.2	0.1	0.0	0.1	0.1	0.1	0.1	0.1	0.1	0.1	0.1	0.1	0.1	0.1	0.0	0.1	0.1	0.1	0.0	0.1	0.1
Cr	0.0	0.0	0.0	0.0	0.0	0.0	0.0	0.0	0.0	0.0	0.0	0.0	0.0	0.0	0.0	0.0	0.0	0.0	0.0	0.0	0.0	0.0	0.0	0.0	0.0	0.0	0.0	0.0	0.0	0.0	0.0	0.0
$Fe^{(II)}$	2.0	2.0	2.1	2.0	2.0	1.8	1.9	2.0	1.8	1.9	1.8	1.9	1.6	1.5	1.6	1.2	1.7	1.7	1.5	1.3	1.2	1.3	1.8	1.3	1.9	1.4	1.5	1.4	1.5	1.3	1.6	1.6
Mn	0.0	0.0	0.0	0.0	0.0	0.0	0.0	0.0	0.0	0.0	0.0	0.0	0.0	0.0	0.0	0.0	0.0	0.0	0.0	0.0	0.0	0.0	0.0	0.0	0.0	0.0	0.0	0.0	0.0	0.0	0.0	0.0
Mg	1.8	1.9	1.8	1.9	1.9	2.0	2.0	1.9	1.9	1.8	1.8	1.8	2.0	2.1	2.2	2.2	2.1	2.1	2.1	2.2	2.3	2.2	2.0	2.2	2.1	2.4	2.2	2.3	2.3	2.3	2.1	2.1
Ca	1.6	1.7	1.6	1.6	1.6	1.6	1.7	1.7	1.6	1.6	1.6	1.6	3.8	3.7	1.7	3.4	1.7	1.7	1.7	3.4	3.4	3.5	1.8	3.5	1.8	3.6	1.7	1.7	1.7	3.5	1.7	1.7
Na	0.6	0.6	0.6	0.7	0.7	0.7	0.6	0.6	0.7	0.6	0.7	0.7	0.6	0.5	0.6	0.4	0.7	0.6	0.6	0.5	0.5	0.4	0.6	0.4	0.6	0.5	0.6	0.6	0.7	0.5	0.7	0.6
K	0.1	0.1	0.1	0.1	0.1	0.1	0.1	0.1	0.1	0.1	0.1	0.1	0.0	0.0	0.1	0.0	0.1	0.1	0.1	0.0	0.0	0.0	0.1	0.0	0.1	0.0	0.1	0.1	0.1	0.0	0.1	0.1
Total	15.3	15.3	15.4	15.4	15.4	15.4	15.4	15.4	15.4	15.3	15.3	15.4	17.4	17.2	15.4	16.8	15.4	15.4	15.4	16.9	16.9	16.9	15.5	16.9	15.5	17.2	15.4	15.4	15.4	17.0	15.4	15.4